

論文 / 著書情報
Article / Book Information

Title	High-Resolution Photoelectron Spectroscopy Study of Degradation of Rubber-to-Brass Adhesion by Thermal Aging
Author	K. Ozawa, T. Kakubo, K. Shimizu, N. Amino, K. Mase, Y. Izumi, T. Muro, T. Komatsu
Journal/Book name	Applied Surface Science, Vol. 268, , pp. 117-123
Issue date	2013, 1
URL	http://www.journals.elsevier.com/applied-surface-science/
DOI	http://dx.doi.org/10.1016/j.apsusc.2012.12.025
Note	このファイルは著者（最終）版です。 This file is author (final) version.

High-Resolution Photoelectron Spectroscopy Study of Degradation of Rubber-to-Brass Adhesion by Thermal Aging

Kenichi Ozawa^{a,*}, Takashi Kakubo^b, Katsunori Shimizu^b, Naoya Amino^b, Kazuhiko Mase^c, Yudai Izumi^d, Takayuki Muro^d, Takayuki Komatsu^a

^a*Department of Chemistry and Materials Science, Tokyo Institute of Technology, Ookayama, Meguro-ku, Tokyo 152-8551, Japan*

^b*The Yokohama Rubber Co., Ltd., Oiwake, Hiratsuka, 254-8601, Japan*

^c*Institute of Materials Structure Science, High Energy Accelerator Research Organization (KEK), Tsukuba 305-0801, Japan*

^d*Japan Synchrotron Radiation Research Institute (JASRI), SPring-8, Sayo, Hyogo 679-5198, Japan*

Abstract

High resolution photoelectron spectroscopy is utilized to investigate degradation of rubber-to-brass adhesion by thermal aging. Special attention is given to the role of water in the environment surrounding brass-embedded rubber so that three aging processes are employed; hydrothermal aging, moist-heat aging and dry-heat aging. All aging processes lead to the decrease in the amount of S at the rubber/brass interface. This desulfurization accompanies the decrease in the ratio of Cu_xS ($x \simeq 2$) to CuS, i.e., $\text{Cu}_x\text{S}/\text{CuS}$, and the increase in the amount of ZnO, $\text{Zn}(\text{OH})_2$ and ZnS, all of which are key factors for degradation of adhesion. The changes in the chemical composition are enhanced by water in the surrounding environment during the aging treatments, indicating that the water molecules accelerate degradation of rubber-to-brass adhesion.

Keywords: Photoelectron spectroscopy, Rubber, Brass, Adhesion, Thermal aging

*Corresponding author. Tel: +81 3 5734 3532; Fax: +81 3 5734 2655
Email address: ozawa.k.ab@m.titech.ac.jp (Kenichi Ozawa)

1. Introduction

Steel-cord-reinforced rubber tires are nowadays a standard type of automotive tires. Strong adhesion between rubber and steel cords is requisite for good performance of tires as well as a prolonged lifetime. To realize strong rubber-to-cord adhesion, the brass-plated steel cords are employed. It has long been recognized that a copper-sulfide layer is formed at the rubber/brass interface, and this interface layer is crucial to realize strong rubber-to-brass adhesion [1–4]. Adhesive properties can be controlled by the vulcanization temperature and time, with a typically condition of 150–180°C for ~ 10 min to obtain good adhesion [5, 6]. The copper-sulfide layer is mainly composed of CuS and Cu_xS with $x \simeq 2$ [7, 8], and Ozawa et al. have revealed in a recent high-resolution photoelectron spectroscopy (PES) study [8] that there is a concentration gradation of both Cu_xS ($x \simeq 2$) and CuS; although CuS is more favored than Cu_xS throughout the entire layer, the concentration of Cu_xS is higher at the rubber side than at the brass side. Since there is a correlation between the concentration of Cu_xS ($x \simeq 2$) and the adhesion strength, Cu_xS rather than CuS is crucial to realize strong interaction between rubber and brass [1, 8].

Long-term usage of the automotive tires induces the loss of the rubber-to-cord adhesion strength. This has been confirmed by accelerated aging tests such as thermal aging and steam aging [2, 5, 6, 9]. One of the proposed degradation mechanisms is the overgrowth of the copper-sulfide layer beyond the optimum thickness [2, 9]. The overgrowth may accompany the transformation of amorphous Cu_xS ($x \simeq 2$) to crystalline one [4], which is brittle and can be easily cleaved, so that the mechanical strength of the adhesive interlayer should be lowered. Accumulation of Zn in the form of ZnO, $\text{Zn}(\text{OH})_2$ and ZnS at the rubber/brass interface is another factor of degradation, because these species bear poor bonding with rubber compounds [1, 3, 9]. The role of iron, which is migrated from steel beneath the brass coating, is also suggested by Patil and van Ooij [10]. Despite the extensive studies, it is still not clear how the chemical composition at the rubber/brass interface is altered during tire aging. The knowledge of the compositional change is important for the development of long-lived tires.

In the present study, we have performed chemical-state analysis of the rubber/brass interface by high-resolution PES to examine the change in the chemical composition induced by three different thermal aging processes, i.e., dry-heat aging, moist-heat aging and hydrothermal aging. It is found that

thermal aging induces the loss of the copper-sulfide species, especially Cu_xS ($x \simeq 2$) and the accumulation of $\text{ZnO}/\text{Zn}(\text{OH})_2$ and ZnS at the interface. Water in the surrounding environment during aging promotes these changes in the chemical composition and thus adhesive degradation.

2. Experimental

Brass plates ($5 \times 5 \times 0.5 \text{ mm}^3$) with a bulk composition of 65 wt% Cu and 35 wt% Zn ($\text{Cu}_{66}\text{Zn}_{34}$; Nilaco Co.) were used as a model sample for a brass-plated steel cord. The sample preparation was the same as that employed in our previous study [8]. Briefly, the brass plates were sandwiched by filter papers and embedded into uncured pads of rubber compounds. Brass-embedded rubber was subjected to vulcanization at 170°C for 10 min under the pressure of 2 MPa. The advantage of the so-called "filter paper method" employed in this study is that chemical reactions equivalent to those at the rubber/brass interface take place on the brass surface while avoiding strong rubber-to-brass adhesion [7, 8]. We also discussed possible drawbacks of this method in our previous paper [8]. The formulation of rubber compounds was as follows; natural rubber (100 phr; parts per hundred rubber), carbon black (60 phr), squalene (10 phr), zinc oxide (10 phr), sulfur (8 phr), cobalt stearate (2 phr), an antioxidant (1 phr) and a curing accelerator (0.5 phr). For details, see Ref. [8].

After vulcanization, thermal aging was conducted at 70°C in three different environmental conditions; one in dry air (dry-heat aging), one in moist air with relative humidity of 96% (moist-heat aging), and one in hot water (hydrothermal aging). The duration of aging was 1 week and 2 weeks. We also prepared unaged samples for comparison.

After the aging treatments, the brass plates were taken out from rubber, placed on sample holders and inserted into the ultrahigh vacuum chambers for the PES measurements. Both synchrotron radiation and laboratory X-ray source were used for the measurements. The synchrotron-radiation PES (SR-PES) measurements were conducted at beam lines (BL) 13A of the Photon Factory, High Energy Accelerator Research Organization (KEK) [11] and BL27SU of SPring-8 [12]. A Gamma Data/Scienta SES200 electron-energy analyzer was used for acquisition of the SR-PES spectra at BL-13A. Typical overall energy resolution was 140 and 250 meV at the photon energies ($h\nu$) of 260 and 1060 eV, respectively. At BL27SU, the SPECS PHOIBOS 150 analyzer was used. The energy resolution was 300 and 350 meV at $h\nu = 260$

Table 1: Influence of thermal aging on the force (N) required to pull the brass-plated steel cords out of cured rubber **and on the rubber coverage (%) on the cords**. The period of aging was 2 weeks.

	Pull-out force (N)	Coverage (%)
Unaged	652	100
Dry-heat aging	566	100
Moist-heat aging	471	75
Hydrothermal aging	350	68

and 1250 eV, respectively. For both systems, the samples were placed so that the sample normal direction was parallel to the lens axes of the analyzers. For the x-ray PES (XPS) measurements, monochromatized Al $K\alpha$ radiation ($h\nu = 1486.6$ eV) was used. A PHI 5000 VersaProbe (ULVAC PHI) analyzer was utilized with an energy resolution of 300 meV. The angle between the lens axis and the sample normal direction was 45° . The electron binding energy of the PES spectra was referenced to the Fermi cut-off in the spectra of the metal plates (Au, Cu or Mo), which were electrically in contact with the brass samples.

In order to evaluate the influence of thermal aging on the rubber-to-brass adhesion strength, forces required to pull brass-plated steel cords out of the rubber compounds were measured. **The cords were constructed by seven filaments (ϕ 0.25 mm) which were helically stranded (a 1×6 structure). The composition of the plated brass film was 63.5 wt% Cu and 36.5 wt% Zn with a mean film thickness of 0.23 μm .** The pull-out test was carried out following the standard test method for adhesion between steel tire cords and rubber (**ASTM D1871**). The steel cords with the embedment length of 12.5 mm were pulled out from rubber, which was cured at 170°C for 10 min and was subjected to two-week-long thermal aging with the same conditions described above.

3. Results

3.1. Pull-out test

Thermal aging is known to reduce the rubber-to-brass adhesion strength. This aging-induced degradation is determined by the pull-out test, in which the forces needed to pull the brass-plated steel cords out of the cured rubber compounds are estimated. The result is shown in Table 1. The pull-out force

of the unaged sample is 652 N, and it is reduced to 566, 471 and 350 N after dry-heat, moist-heat and hydrothermal aging for 2 weeks, respectively. The force is diminished as the content of water in the surrounding environment during thermal aging is increased. In Table 1, the coverage of rubber, which remains on the cord surfaces after pulled out, are also shown. The decrease in the coverage with the water content is an another indication of degradation of adhesion. The negative influence of humidity on the adhesion strength has already been pointed out by Van Ooij [2], Jeon and Seo [5, 6] and Buytaert et al [9]. The result of the pull-out test clearly demonstrates that the water molecules in the surrounding environment accelerate adhesion degradation during thermal aging. On the basis of the PES measurements, we show in the following sections that there is a good correlation between water-stimulated degradation and the chemical composition at the rubber/brass interface.

3.2. Hydrothermal aging

Fig. 1 shows XPS spectra of the vulcanized brass surfaces subjected to hydrothermal aging for 0 (unaged), 1 and 2 weeks. Peaks associated with Cu (Cu $2p_{3/2}$ and $2p_{1/2}$ at 932 and 952 eV, respectively, Cu LMM at 568 eV, and Cu 3p at 75 eV), C (C 1s at 284 eV), S (S 2s at 226 eV and S 2p at 162 eV) are observed as major peaks on the unaged surface (a bottom curve). The O 1s peak (532 eV) and the Zn 2p peak (1022 eV for $2p_{3/2}$) are also observable with weak intensities, indicating low densities of O and Zn on the vulcanized brass surfaces. This agrees well with our previous work [8].

Hydrothermal aging results in a decrease in the amount of interfacial S, while the atomic densities of Zn and O are in an increasing trend with time. The inset of Fig. 1 shows the change in the relative atomic densities of the major elements on the brass surface as a function of aging time. The S atomic density is decreased to 60–70% of the unaged value by hydrothermal aging for 1 and 2 weeks. The decrease in the S density means desulfurization at the brass surface. This process accompanies the increase in the Zn and O atomic densities; approximately 10-fold and 2.5-fold increases are observed for the Zn and O densities, respectively. Formation of ZnO and/or Zn(OH)₂, which are not distinguished by the present PES measurements, is a probable cause of the increase in the Zn and O densities [2, 3, 9]. In our recent study, we have found that a similar change in the chemical composition is also induced by prolonged vulcanization at 170°C [8]. Thus, influence of thermal aging on the chemical composition at the rubber-brass interface should be similar to that of prolonged vulcanization at a much higher temperature.

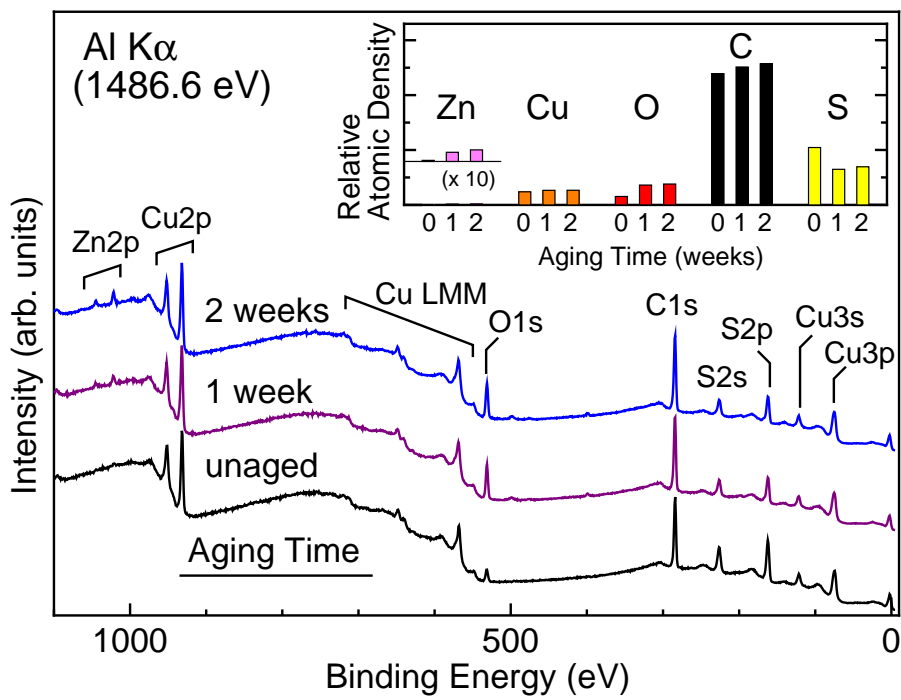


Figure 1: XPS spectra of the vulcanized brass samples subjected to hydrothermal aging for 0 (unaged), 1 and 2 weeks. The inset shows relative atomic densities of the major elements on the surfaces. The densities are obtained from the integrated intensities of the core-level peaks (Zn 2p, Cu 2p, O 1s, C 1s and S 2p) and their photoionization cross sections [13].

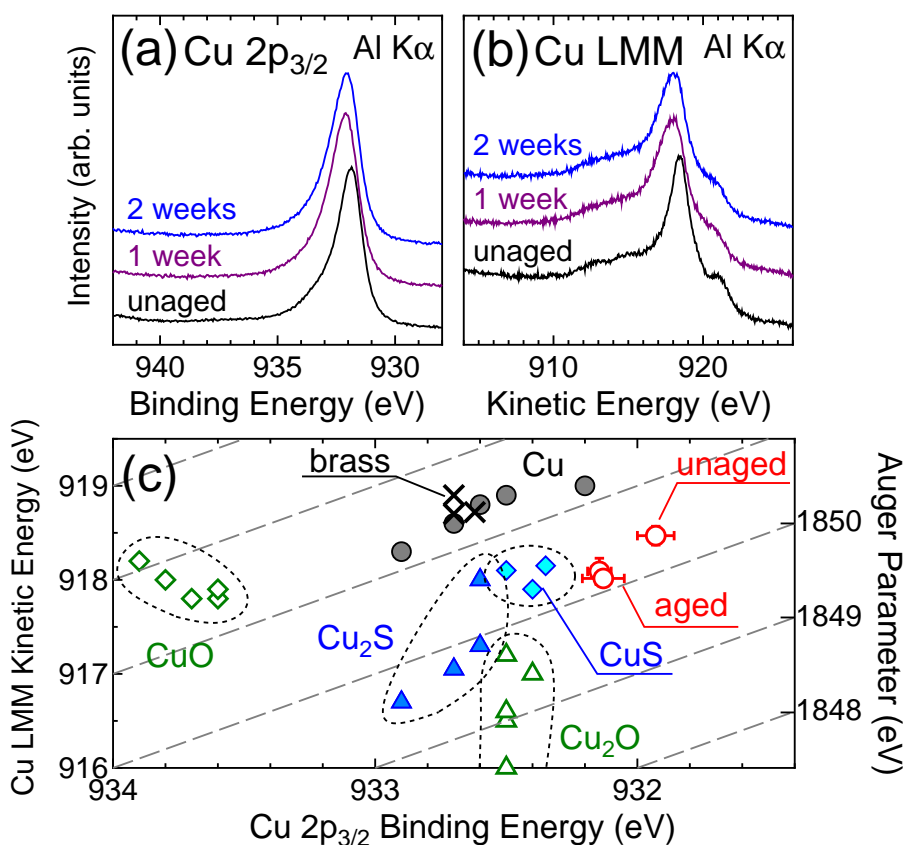


Figure 2: XPS spectra in (a) Cu 2p_{3/2} core-level and (b) Cu LMM Auger electron emission regions. The photon energy is 1486.6 eV (Al K α). (c) Wagner plot for various Cu-containing species; metallic Cu (filled circles) [14–18], brass (\times) [8, 14, 19], Cu₂O (open triangles) and CuO (open diamonds) [14, 15, 17–20], Cu₂S (filled triangles) and CuS (filled diamonds) [14, 17, 21, 22], and unaged and aged (1 and 2 weeks) brass samples examined in the present study (open circles with error bars).

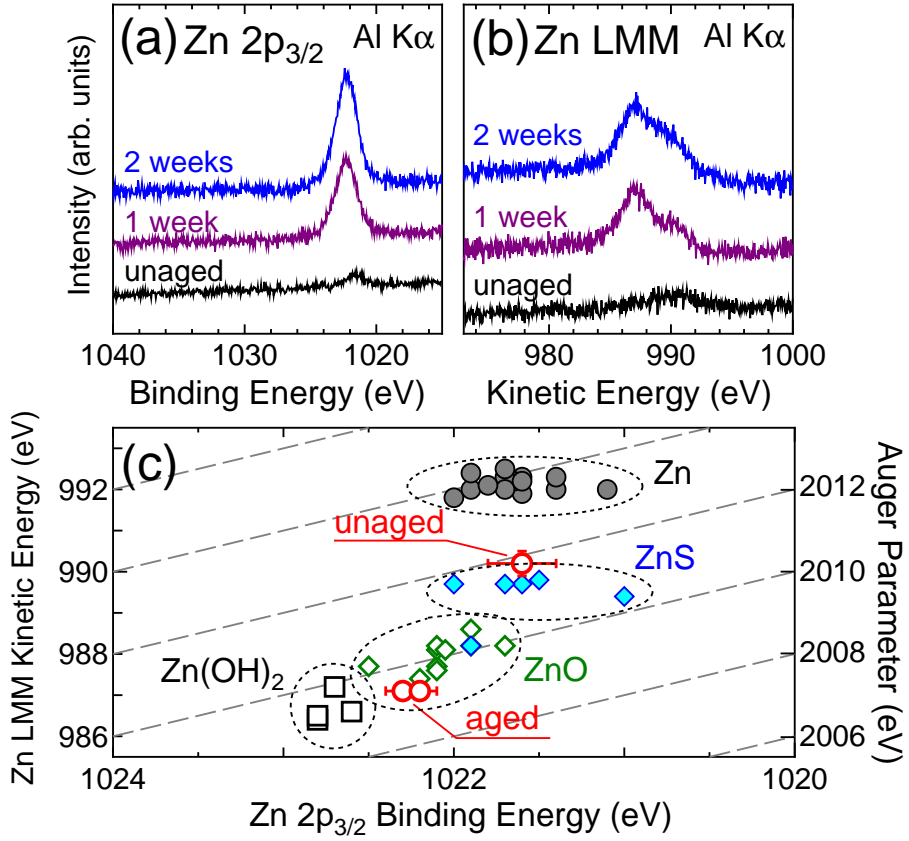


Figure 3: XPS spectra in (a) Zn 2p_{3/2} core-level and (b) Zn LMM Auger electron emission regions. The photon energy is 1486.6 eV (Al K α). (c) Wagner plot for various Zn-containing species; metallic Zn (filled circles) [14, 23, 24], ZnS (filled diamonds) [14, 23, 24], ZnO (open diamonds) [14, 23–25], Zn(OH)₂ [14, 23, 25], and unaged and aged (1 and 2 weeks) brass samples examined in the present study (open circles with error bars).

In order to obtain detailed picture of the change in the chemical states of the composite elements upon aging, we first examined the Cu- and Zn-related peaks. Figs. 2a and 2b show the Cu $2p_{3/2}$ core-level and Cu LMM Auger electron spectra. On the unaged surface, the Cu $2p_{3/2}$ and Cu LMM peaks are observed at 931.9 eV in binding energy and 918.5 eV in kinetic energy, respectively. Hydrothermal aging leads to the shift of both peaks towards higher binding energies (lower kinetic energies). A Wagner plot in Fig. 2c shows that the data point of the unaged sample do not fall in the regions of any of the Cu-related species, but the Auger parameter of 1850.4 eV suggests CuS-like species as main Cu-related species. The data points of the aged samples are close to the CuS region with the Auger parameter of ~ 1850.2 eV. Thus, a more CuS-rich environment is realized by hydrothermal aging.

Figs. 3a and 3b depict the Zn $2p_{3/2}$ core-level and Zn LMM Auger electron spectra. Because the vulcanized brass surface is entirely covered with the copper-sulfide layer [8], the Zn-related peaks are observed as weak peaks on the unaged surface. Thermal aging induces the growth of both Zn $2p$ and Zn LMM peaks along with the energy shift towards the higher binding (lower kinetic) energy side. The Wagner plot (Fig. 3c) clearly indicates that the Zn atoms exist in the copper-sulfide layer in the form of ZnS on the brass surface after vulcanization, while the main Zn-containing species become ZnO with a possible contribution of Zn(OH)₂ after hydrothermal aging. The increase in the amount of ZnO/Zn(OH)₂ means that dezincification of brass proceeds on the sulfurized surface during aging [3].

Figs. 4a and 4b show S $2p$ core-level spectra measured with synchrotron radiation light ($h\nu = 260$ and 1060 eV, respectively). The spectra measured with $h\nu = 260$ eV is more surface sensitive than those measured with $h\nu = 1060$ eV, because the escape depths are 0.4–0.55 nm (260 eV) and 1.5–2.8 nm (1060 eV) [8]. Since several S-containing species exist on the vulcanized brass surface, the spectral lineshape is complex enough not to allow us a simple interpretation. Thus, a lineshape analysis was conducted with the same procedure as that employed in our previous study [8]. Each S $2p$ spectrum is decomposed into five components, i.e., CuS, Cu_xS ($x \simeq 2$), S in S-rich environment, polysulfides including octasulfur, and ZnS and/or precursor states to copper sulfides. The emission peak from the polysulfides is dominant in the S $2p$ spectrum of the unaged brass sample measured with $h\nu = 260$ eV, indicating the accumulation of polysulfides on the surface during vulcanization. The complex feature at the lower binding energy side

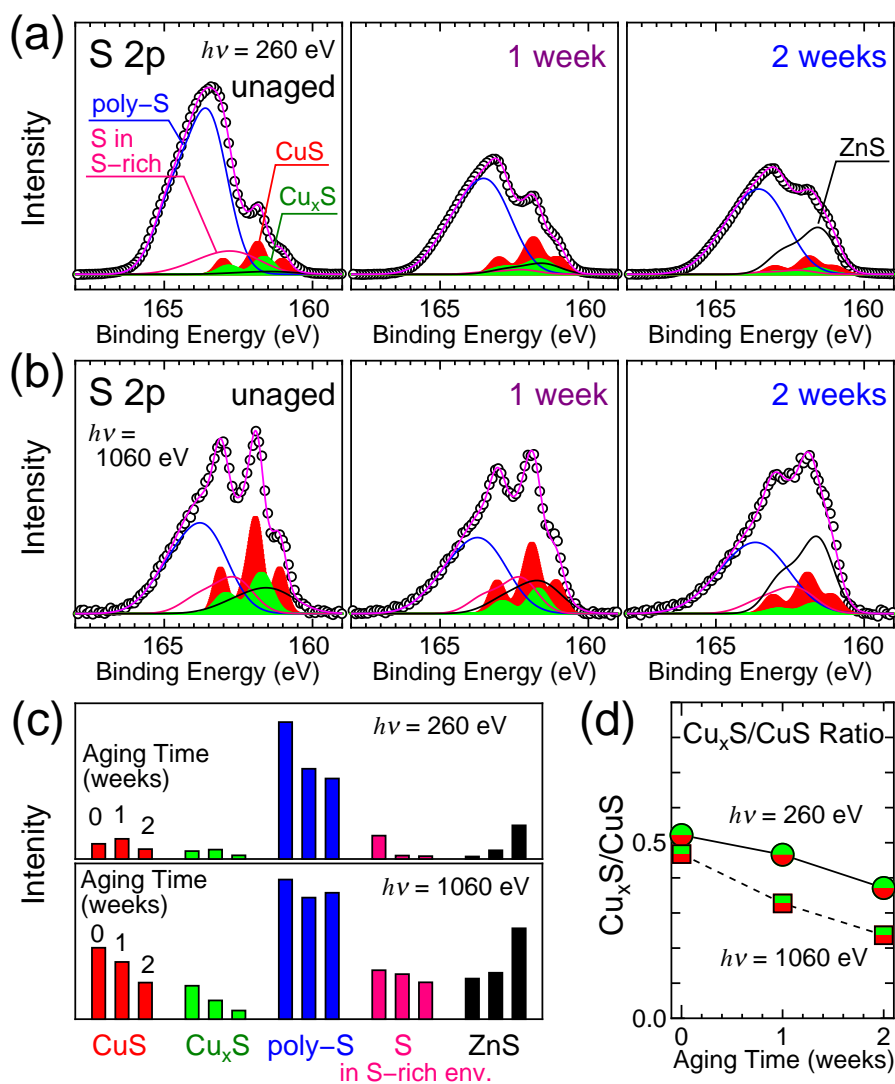


Figure 4: S 2p SR-PES spectra of vulcanized brass surfaces subjected to hydrothermal aging for 0 (unaged), 1 and 2 weeks. The photon energies are (a) 260 eV and (b) 1060 eV. Curves drawn by circles are the measured spectra after Shirley-type backgrounds are subtracted. Solid lines are the results of peak deconvolution. (c) Change in the integrated intensity of each S 2p component from a S-containing species as a function of hydrothermal aging time. (d) Change in the intensity ratio of the S 2p peaks from Cu_xS ($x \simeq 2$) and CuS as a function of the aging time. Circles and squares are the data from the spectra measured with $h\nu = 260$ eV and 1060 eV, respectively.

(160–163 eV) is owing to the emission from CuS and Cu_xS ($x \simeq 2$).

Hydrothermal aging induces desulfurization at the brass surface (Fig. 1), and the lineshape analysis of the S 2p spectra reveals that the decrease in the amount of polysulfides is the main reason for desulfurization. Other noticeable changes are the decrease in the amount of the copper sulfides [CuS and Cu_xS ($x \simeq 2$)] and the increase in the amount of ZnS and/or the precursor to the copper sulfides. Because the aging treatment results in the increase in the amount of Zn (Fig. 1), accumulation of ZnS rather than the precursor states should be a probable consequence of aging. Although we draw the conclusion on the basis of Fig. 3c that ZnO/Zn(OH)₂ is the main products as the Zn-containing species, ZnS should also be formed and accumulated in the surface region during hydrothermal aging. The aging-time dependence of the amounts of the S-containing species is indicated in Fig. 4c.

It is known that the copper sulfides, especially Cu_xS ($x \simeq 2$), is crucial for strong rubber-to-brass adhesion [1]. Fig. 3d shows the change in the ratio of the copper sulfides, i.e., $\text{Cu}_x\text{S}/\text{CuS}$, as a function of the aging time. The $\text{Cu}_x\text{S}/\text{CuS}$ values are decreased with time, indicating that the copper-sulfide layer becomes more CuS-rich environment so that rubber-to-brass adhesion must be degraded. Moreover, the increase in the amounts of ZnO/Zn(OH)₂ and ZnS by hydrothermal aging also contributes to weakening of the rubber-to-brass bonding because these species are not good agents for adhesion [1, 3]. In the next section, we show that water in the surrounding environment during the aging treatment plays a crucial role in the adhesion degradation process.

3.3. Moist-heat and dry-heat aging

In the aging process of rubber-to-brass adhesion, humidity in the surrounding environment often affects the degree of degradation [2, 5, 6, 9]. To reveal the role of water in the aging process, the amount of water in the surrounding environment was controlled during thermal aging (70°C), and the chemical composition at the rubber/brass interface was examined.

The most affected chemical species by surrounding water are the S-containing species. Figs. 5a and 5b show the S 2p spectra of the vulcanized brass surfaces after dry-heat and moist-heat aging, respectively. Both aging treatments lead to a decrease in the S 2p spectral intensities, indicating aging-induced desulfurization at the rubber/brass interface.

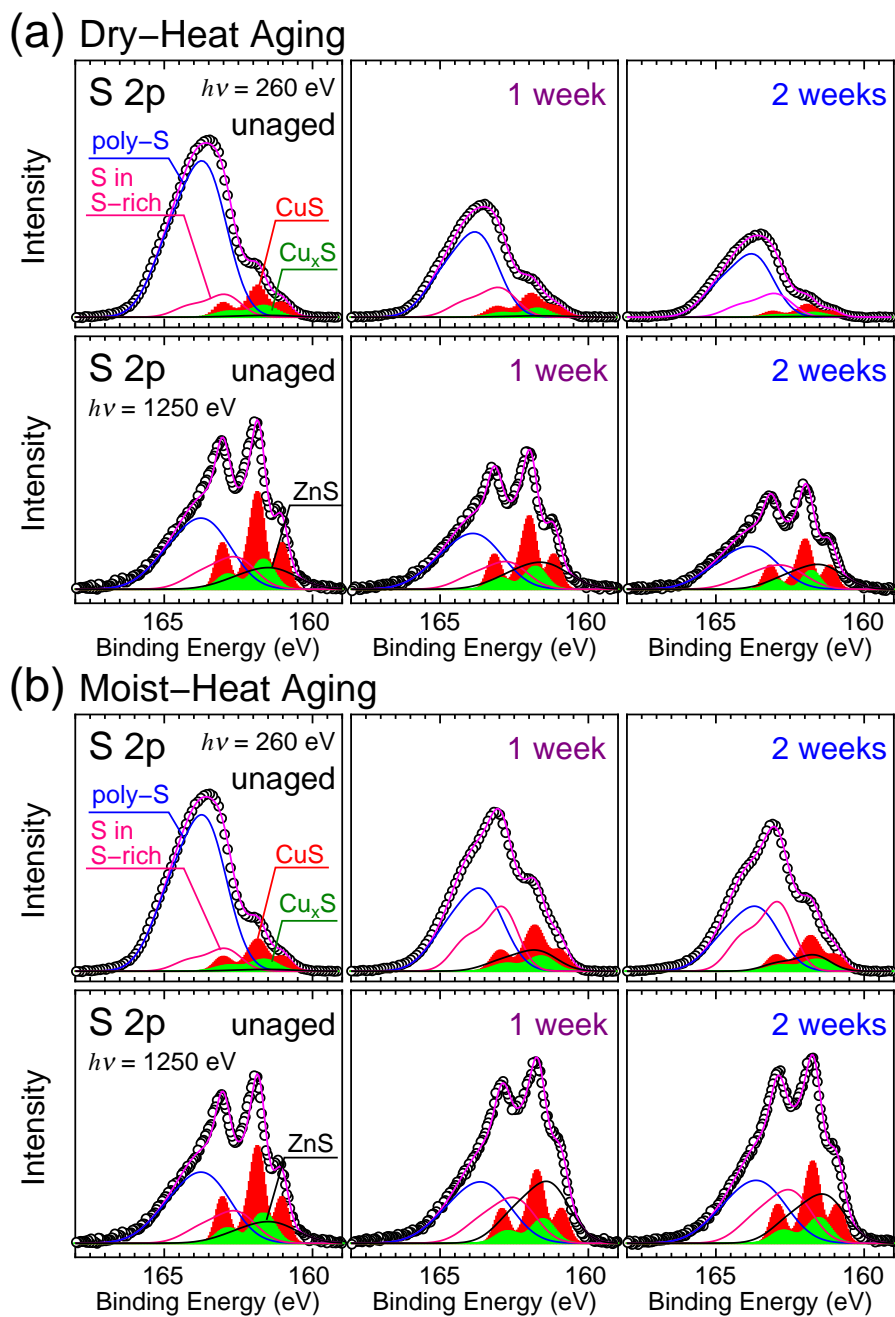
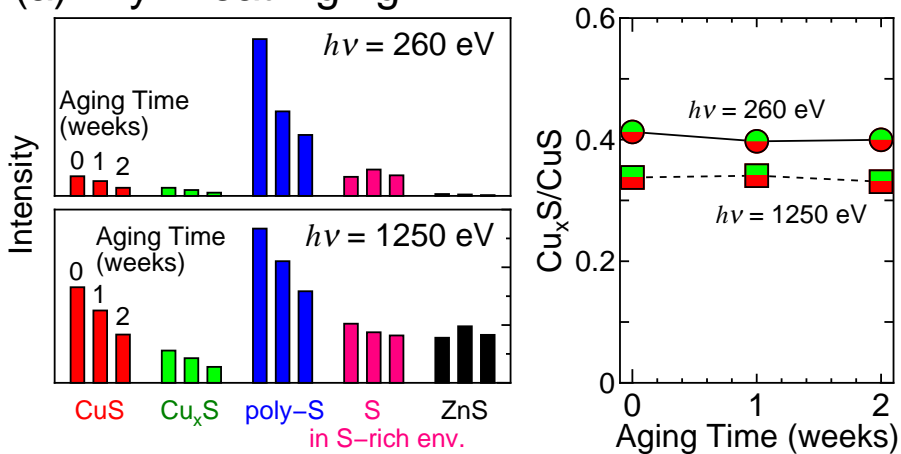


Figure 5: S 2p SR-PES spectra of vulcanized brass surfaces subjected to (a) dry-heat aging and (b) moist-heat aging for 0, 1 and 2 weeks. The spectra in the upper and lower panels in Figs. 4a and 4b are measured with $h\nu = 260$ eV and 1250 eV, respectively.

(a) Dry-Heat Aging



(b) Moist-Heat Aging

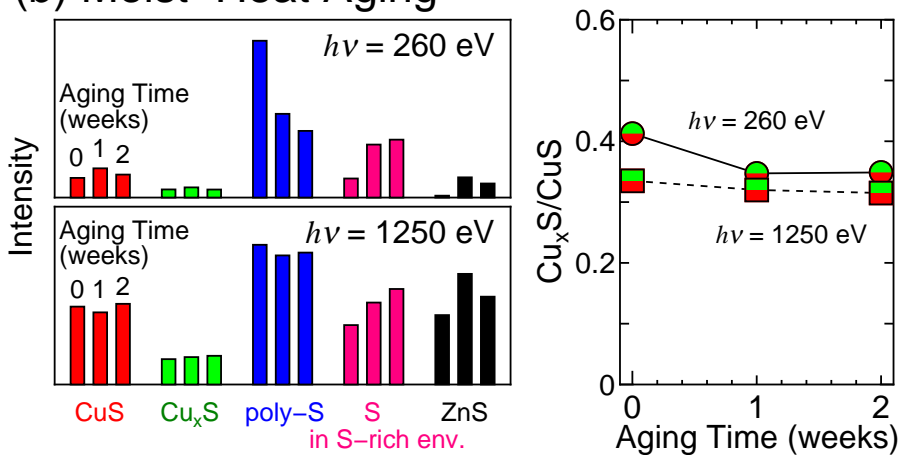


Figure 6: Changes in the integrated intensity of each S 2p component from a S-containing species (left panels) and the $\text{Cu}_x\text{S}/\text{CuS}$ ratio ($x \simeq 2$) as a function of the aging time (right panels). Upper and lower panels are the results of (a) dry-heat aging and (b) moist-heat aging, respectively.

Apart from the intensity variation, one can notice that the different aging treatments lead to a different change in the S 2p lineshape. As shown in the previous section, hydrothermal aging induces a drastic change in the spectral lineshape as a result of the large compositional change of the S-containing species (Fig. 4). On the other hand, except for the diminishment of the intensity, the S 2p lineshape is nearly the same in the case of dry-heat aging (Fig. 5a). This means that dry-heat aging do not affect the relative composition of the S-containing species. The spectral change by moist-heat aging (Fig. 5b) is in between hydrothermal aging and dry-heat aging. The notable feature of the influence of moist-heat aging is that the slight increase in the amounts of CuS and Cu_xS ($x \simeq 2$) as shown in the left panels in Fig. 6b. However, the $\text{Cu}_x\text{S}/\text{CuS}$ ratio is diminished with aging time (the right panel in Fig. 6b). This suggests the steady progress of degradation of adhesion. In moist aging, the increase in the amount of ZnS is recognized, and this also contributes to adhesive degradation.

Since dry-heat aging does not affect the relative composition of the S-containing species at the rubber/brass interface, the $\text{Cu}_x\text{S}/\text{CuS}$ ratio is nearly constant with aging time (the right panel in Fig. 6a). Moreover, the amount of ZnS in the surface region is kept low even after dry-heat aging (see the upper left panel in Fig. 6a). Thus, degradation of adhesion must be limited by dry-heat aging.

4. Discussion

Thermal aging of brass-embedded rubber induces the changes in the chemical composition at the rubber/brass interface. The decrease in the amount of sulfur, i.e., desulfurization, is one of the consequence of thermal aging. It has been recognized that thermal aging leads to thickening of the adhesion layer composed of the sulfides (CuS, Cu_xS and ZnS) [2, 9, 26]. Desulfurization and layer thickening seem to be inconsistent with each other. However, such an inconsistency should arise from the difference in the thickness of the region considered; the probing depth of the brass surface in the present PES measurements is less than several nanometers, whereas the thickness of the sulfide layer is several tens of nanometers [5, 6, 26]. Therefore, we consider that thermal aging induces thickening of the sulfide layer along with the decrease in the S density on the very surface of the brass samples.

Thermally-induced desulfurization accompanies the increase in the amounts of $\text{ZnO}/\text{Zn}(\text{OH})_2$ and ZnS and the decrease in the ratio of $\text{Cu}_x\text{S}/\text{CuS}$, both of

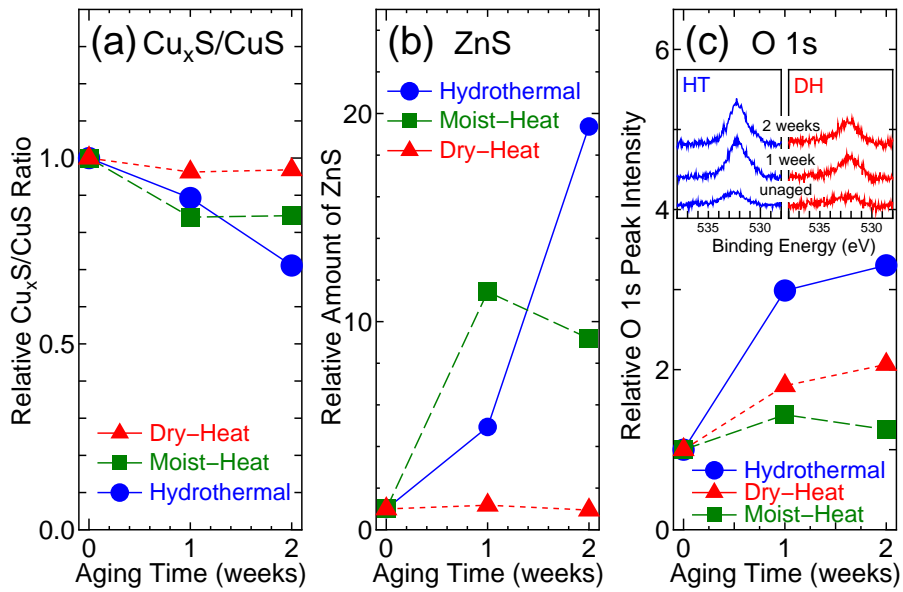


Figure 7: Influence of different aging treatments on (a) the $\text{Cu}_x\text{S}/\text{CuS}$ ratio ($x \simeq 2$), (b) the amount of ZnS and (c) the O 1s peak intensity. The values of the unaged sample are taken as unity so as easily to compare the changes depending on different aging treatments. The data of $\text{Cu}_x\text{S}/\text{CuS}$ and ZnS are deduced from the S 2p spectra measured with $h\nu = 260$ eV. The O 1s peak intensities are determined from the spectra measured with $h\nu = 1060$ eV for hydrothermal aging and 1250 eV for moist- and dry-heat aging. The inset of Fig. 6c show the O 1s spectra of the brass samples subjected to hydrothermal aging (left) and dry-heat aging (right).

which reflect degradation of adhesion. The present study clearly shows that water in the surrounding environment during the aging treatments enhances these changes and, thus, promotes degradation of rubber-to-brass adhesion. In Figs. 7a and 7b, we compare the aging-time dependence of the $\text{Cu}_x\text{S}/\text{CuS}$ ratio and the amount of ZnS obtained from the S 2p spectra measured with $h\nu = 260$ eV. The values of the unaged samples are taken as unity so as easily to compare the variation with aging time in different aging treatment. Although the data points are scattered rather widely, a clear tendency is recognized; as the water content in the surrounding environment is higher, larger decrease and increase in $\text{Cu}_x\text{S}/\text{CuS}$ and ZnS, respectively, are induced. This trend correlates with the amount of the O atoms on the brass surfaces. Fig. 7c shows the O 1s peak intensities, which are normalized by the O 1s peak intensities of the unaged samples. The O atoms on the brass surface are populated after all thermal aging treatments, but with a higher increasing rate on the hydrothermally-aged brass sample than those on the dry-heat and moist-heat aged samples. This suggests that the O atoms should play roles to stimulate degradation of adhesion at the rubber/brass interface.

We speculate that the increase in the O density on the brass surface must result from infiltration of water and/or O_2 in the surrounding environment into rubber during thermal aging. Because there is a correlation between the aging-induced changes and the amount of water in the environment, water must be a more important than O_2 for degradation of adhesion. To prove water infiltration during thermal aging, the O density in the rubber compound was examined before and after hydrothermal aging. Rubber pieces with the size of $5 \times 5 \times 0.5$ mm³ were sliced out from the blocks of rubber, and the several areas on the rubber pieces were measured by XPS. Note that all measured areas were not exposed to air or water during hydrothermal aging. Fig. 8 shows the typical O 1s spectra of the unaged and 2-week-long hydrothermally-aged rubber pieces. The O 1s peak with a larger intensity is observed on aged rubber. The oxygen-to-carbon (O/C) atomic ratio is 0.018 before aging and is increased to 0.023 after aging (the inset of Fig. 8). Thus, the aging treatment results in the increase in the density of the O atoms in rubber. Each O 1s peak is reproduced by a single Gaussian peak with its peak position at 531.3 eV, which is attributed neither to H_2O (533 eV [27]) nor to OH (532.6–532.7 eV [28]) but to a C=O group (532 eV [28]). Thus, H_2O should be decomposed upon infiltration into rubber and migrate in the decomposed form in rubber to reach the rubber/brass interface.

The O atoms accumulated on the brass surface have two important roles

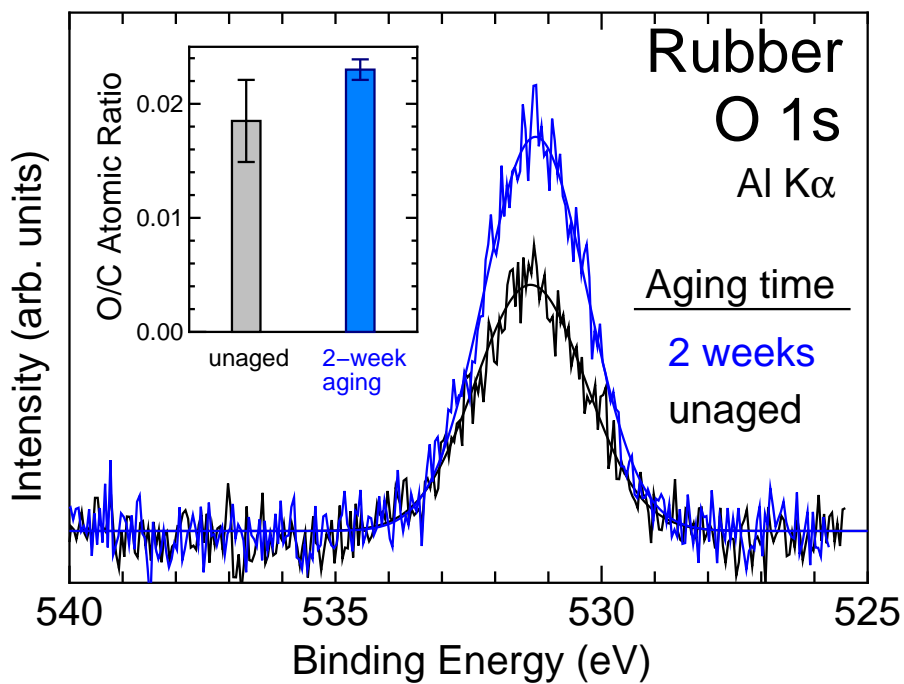


Figure 8: The O 1s XPS spectra of unaged and hydrothermal-aged rubber. A Shirley-type background curve is subtracted from each measured spectra. Although low energy electrons and argon ions were irradiated to avoid possible charging during data acquisition, small shifts by charging was observed. Thus, the C 1s peak position at 283.9 eV, which is obtained from rubber with sufficient conductivity by adding carbon black of the amount of 100 phr, is taken as a reference point of the binding energy. The inset shows the O atomic densities normalized by the C atomic densities for the unaged and aged rubber samples.

to weaken interface adhesion. One is to induce desulfurization reactions of the copper sulfides via $\text{Cu}_x\text{S} + \text{O} \rightarrow \text{Cu}_x\text{O} + \text{S}$ ($x = 1 - 2$). Such oxidative desulfurization is indeed operative when S-containing copper is desulfurized in the presence of O [29]. The other is to stimulate the dezincification process of brass, i.e. the formation process of ZnO and $\text{Zn}(\text{OH})_2$. Because of large electronegativity of O, the O atoms on top of the adhesion layer should be negatively charged. This negative charge is a driving force to accelerate the Zn^{2+} diffusion from the ZnO layer and brass below the adhesion layer, i.e., the anode side of the adhesion layer, and ZnO and $\text{Zn}(\text{OH})_2$ are formed as a result [3]. Although the O atoms are not directly involved in the formation of ZnS, they also stimulate the formation of ZnS by the reaction; $\text{Cu}_x\text{S} + \text{Zn} \rightarrow \text{ZnS} + x\text{Cu}$.

Finally, we give a short comment on the role of cobalt on the bonding between rubber and brass. As one of various additives, organic cobalt compounds are added to tire rubber for the promotion of rubber-to-brass adhesion and the prevention of adhesion degradation [30]. In the present study, rubber containing cobalt stearate with 2 phr is used. However, our PES measurements reveal that the density of the cobalt compound is below the detection limit on the brass surface. This suggests that a direct involvement of cobalt in the rubber-brass bond formation should be minor even if exists. At present, the function of cobalt still remains unanswered, although there are numerous preceding studies [30]. Thus, further studies are required on this topic to understand how cobalt works in rubber as well as at the interface as a first step to replace cobalt-containing compounds with a heavy-metal-free ones to reduce environmental impact.

5. Summary

High resolution photoelectron spectroscopy is utilized to investigate degradation of rubber-to-brass adhesion by thermal aging at 70°C. Special attention is given to the role of water in the environment surrounding brass-embedded rubber so that three aging processes are employed; hydrothermal aging, moist-heat aging and dry-heat aging. All aging processes lead to the decrease in the amount of S at the rubber/brass interface, i.e., desulfurization of the adhesive interlayer is induced. This desulfurization accompanies the decrease in the ratio of $\text{Cu}_x\text{S}/\text{CuS}$ ($x \simeq 2$) as well as the increase in the amounts of ZnO, $\text{Zn}(\text{OH})_2$ and ZnS, all of which are key factors for degradation of adhesion. The aging-induced changes are correlated with the content

of water in the environment surrounding brass-embedded rubber during the aging treatments. The water molecules are infiltrated into rubber to increase in the density of O in rubber as well as on the brass surface. The O atoms promote decomposition of the copper sulfides and the increase in ZnO, Zn(OH)₂ and ZnS. Thus, humidity accelerates weakening of the rubber-to-brass bonding.

6. Acknowledgement

The PES measurements using synchrotron radiation at the Photon Factory and SPring-8 were performed under approvals of the Photon Factory Advisory Committee (Proposal No. 2010G550) and the SPring-8 Advisory Committee (No. 2011A1770).

References

- [1] W.J. van Ooij, *Surface Science* 68 (1977) 1.
- [2] W.J. van Ooij, *Rubber Chemistry and Technology* 52 (1979) 605.
- [3] W.J. van Ooij, *Rubber Chemistry and Technology* 57 (1984) 421.
- [4] W.J. van Ooij, P.B. Harakuni, *Rubber Chemistry and Technology* 82 (2009) 315.
- [5] G.S. Jeon, G. Seo, *Journal of Adhesion* 76 (2001) 201.
- [6] G.S. Jeon, G. Seo, *Journal of Adhesion* 76 (2001) 223.
- [7] T. Hokata, Y. Ishikawa, K. Mori, *Rubber Chemistry and Technology* 80 (2007) 61.
- [8] K. Ozawa, T. Kakubo, K. Shimizu, N. Amino, K. Mase, T. Komatsu, *Applied Surface Science*, submitted.
- [9] G. Buytaert, H. Kiang, G. Pax, P. Reis, *Rubber and Plastics News*, November 29 (2010) 14.
- [10] P.Y. Patil, W.J. van Ooij, *Journal of Adhesion Science and Technology* 18 (2004) 1367.
- [11] A. Toyoshima, H. Tanaka, T. Kikuchi, K. Amemiya, K. Mase, *Journal of the Vacuum Society of Japan* 54 (2011) 580.
- [12] H. Ohashia, E. Ishigurob, Y. Tamenoria, H. Kishimotoa, M. Tanakaa, M. Iriea, T. Tanakaa, T. Ishikawaa, *Nuclear Instruments and Methods in Physics Research A*, 467-468 (2001) 533.
- [13] J.J. Yeh, I. Lindau, *Atomic Data and Nuclear Data Tables* 32 (1985) 1.
- [14] G. Deroubaix, P. Marcus, *Surface and Interface Analysis* 18 (1992) 39.
- [15] W.J. van Ooij, *Surface Technology* 6 (1977) 1.
- [16] C. Battistoni, G. Mattogno, E. Paparazzo, L. Naldini, *Inorganic Chimica Acta* 102 (1985) 1.

- [17] S.K. Chawla, N. Sankarraman, J.H. Payer, *Journal of Electron Spectroscopy and Related Phenomena* 61 (1992) 1.
- [18] V. Hayez, A. Fracquet, A. Hubin, H. Terry, *Surface and Interface Analysis* 36 (2004) 876.
- [19] S. Maroie, G. Haemers, J.J. Verbist, *Applied Surface Science* 17 (1984) 463.
- [20] A. Laufer, D. Reppin, H. Metelmann, S. Geburt, C. Ronning, T. Leichtweiss, J. Janek, B.K. Meyer, *Physica Status Solidi (b)* 249 (2012) 801.
- [21] D.L. Perry, J.A. Taylor, *Journal of Materials Science Letters* 5 (1986) 384.
- [22] M. Kundu, T. Hasegawa, K. Terabe, K. Yamamoto, M. Aono, *Science and Technology of Advanced Materials* 9 (2008) 035011.
- [23] L.S. Dake, D.R. Baer, J.M. Zachara, *Surface and Interface Analysis* 14 (1989) 71.
- [24] S.W. Gaarenstroom, N. Winograd, *Journal of Chemical Physics* 67 (1977) 3500.
- [25] W. Fürbeth, M. Stratmann, *Corrosion Science* 43 (2001) 207.
- [26] G.E. Hammer, *Journal of Vacuum Science and Technology A* 19 (2001) 2846.
- [27] M.A. Henderson, *Surface Science Report*. 46 (2002) 1.
- [28] A. Rjeb, S. Letarte, L. Tajounte, M. Chafik El Idrissi, A. Adnot, D. Roy, Y. Clire, J. Kaloustian, *Journal of Electron Spectroscopy and Related Phenomena* 107 (2000) 221.
- [29] Y. Fukunaka, K. Nishikawa, H.S. Sohn, Z. Asaki, *Metallurgical Transactions B* 22 (1991) 5.
- [30] **W.S. Fulton, *Rubber Chemistry and Technology* 78 (2005) 426.**

Table captions

Influence of thermal aging on the force (N) required to pull the brass-plated steel cords out of cured rubber **and on the rubber coverage (%) on the cords**. The period of aging was 2 weeks.

Figure captions

Figure 1: XPS spectra of the vulcanized brass samples subjected to hydrothermal aging for 0 (unaged), 1 and 2 weeks. The inset shows relative atomic densities of the major elements on the surfaces. The densities are obtained from the integrated intensities of the core-level peaks (Zn 2p, Cu 2p, O 1s, C 1s and S 2p) and their photoionization cross sections [13].

Figure 2: XPS spectra in (a) Cu $2p_{3/2}$ core-level and (b) Cu LMM Auger electron emission regions. The photon energy is 1486.6 eV (Al $K\alpha$). (c) Wagner plot for various Cu-containing species; metallic Cu (filled circles) [14–18], brass (\times) [8, 14, 19], Cu_2O (open triangles) and CuO (open diamonds) [14, 15, 17–20], Cu_2S (filled triangles) and CuS (filled diamonds) [14, 17, 21, 22], and unaged and aged (1 and 2 weeks) brass samples examined in the present study (open circles with error bars).

Figure 3: XPS spectra in (a) Zn $2p_{3/2}$ core-level and (b) Zn LMM Auger electron emission regions. The photon energy is 1486.6 eV (Al $K\alpha$). (c) Wagner plot for various Zn-containing species; metallic Zn (filled circles) [14, 23, 24], ZnS (filled diamonds) [14, 23, 24], ZnO (open diamonds) [14, 23–25], $\text{Zn}(\text{OH})_2$ [14, 23, 25], and unaged and aged (1 and 2 weeks) brass samples examined in the present study (open circles with error bars).

Figure 4: S 2p SR-PES spectra of vulcanized brass surfaces subjected to hydrothermal aging for 0 (unaged), 1 and 2 weeks. The photon energies are (a) 260 eV and (b) 1060 eV. Curves drawn by circles are the measured spectra after Shirley-type backgrounds are subtracted. Solid lines are the results of peak deconvolution. (c) Change in the integrated intensity of each S 2p component from a S-containing species as a function of hydrothermal aging time. (d) Change in the intensity ratio of the S 2p peaks from Cu_xS

($x \simeq 2$) and CuS as a function of the aging time. Circles and squares are the data from the spectra measured with $h\nu = 260$ eV and 1060 eV, respectively.

Figure 5: S 2p SR-PES spectra of vulcanized brass surfaces subjected to (a) dry-heat aging and (b) moist-heat aging for 0, 1 and 2 weeks. The spectra in the upper and lower panels in Figs. 4a and 4b are measured with $h\nu = 260$ eV and 1250 eV, respectively.

Figure 6: Changes in the integrated intensity of each S 2p component from a S-containing species (left panels) and the $\text{Cu}_x\text{S}/\text{CuS}$ ratio ($x \simeq 2$) as a function of the aging time (right panels). Upper and lower panels are the results of (a) dry-heat aging and (b) moist-heat aging, respectively.

Figure 7: Influence of different aging treatments on (a) the $\text{Cu}_x\text{S}/\text{CuS}$ ratio ($x \simeq 2$), (b) the amount of ZnS and (c) the O 1s peak intensity. The values of the unaged sample are taken as unity so as easily to compare the changes depending on different aging treatments. The data of $\text{Cu}_x\text{S}/\text{CuS}$ and ZnS are deduced from the S 2p spectra measured with $h\nu = 260$ eV. The O 1s peak intensities are determined from the spectra measured with $h\nu = 1060$ eV for hydrothermal aging and 1250 eV for moist- and dry-heat aging. The inset of Fig. 6c show the O 1s spectra of the brass samples subjected to hydrothermal aging (left) and dry-heat aging (right).

Figure 8: The O 1s XPS spectra of unaged and hydrothermal-aged rubber. A Shirley-type background curve is subtracted from each measured spectra. Although low energy electrons and Ar^+ were irradiated to avoid possible charging during data acquisition, small shifts by charging was observed. Thus, the C 1s peak positions at 283.9 eV, which is obtained from rubber with sufficient conductivity by adding carbon black of the amount of 100 phr is taken as a reference point of the binding energy. The inset shows the O atomic densities normalized by the C atomic densities for the unaged and aged rubber samples.